Received: 28 February 2018 | Accepted: 13 June 2018

DOI: 10.1002/jcp.26900

ORIGINAL RESEARCH ARTICLE

WILEY Journal of Cellular Physiology

Epigallocatechin gallate in combination with eugenol or amarogentin shows synergistic chemotherapeutic potential in cervical cancer cell line

Debolina Pal[1] | Subhayan Sur[1] | Rituparna Roy[1] | Suvra Mandal[2] | Chinmay Kumar Panda[1]

[1]Department of Oncogene Regulation, Chittarangan National Cancer Institute, Kolkata, India

[2]Department of Chemistry, National Research Institute for Ayurvedic Drug Development, Kolkata, India

Correspondence
Department of Oncogene Regulation, Chittaranjan National Cancer Institute, 37, S.P. Mukherjee Road, Kolkata 700026, India.
Email: ckpanda.cnci@gmail.com

Funding information
CSIR fellowship for Research Associate (RA), Grant/Award Number: 09/030(0074)/2014 EMR-I

In this study, antitumor activity of epigallocatechin gallate (EGCG; major component of green tea polyphenol), eugenol (active component of clove), and amarogentin (active component of chirata plant) either alone or in combination were evaluated in Hela cell line. It was evident that EGCG with eugenol–amrogentin could highly inhibit the cellular proliferation and colony formation than individual treatments. Induction of apoptosis was also higher after treatment with EGCG in combination with eugenol–amrogentin than individual compound treatments. The antiproliferative effect of these compounds was due to downregulation of cyclinD1 and upregulation of cell cycle inhibitors LIMD1, RBSP3, and p16 at G1/S phase of cell cycle. Treatment of these compounds could induce promoter hypomethylation of LimD1 and P16 genes as a result of reduced expression of DNA methyltransferase 1 (DNMT1). Thus, our study indicated the better chemotherapeutic effect of EGCG in combination with eugenol–amarogentin in Hela cell line. The chemotherapeutic effect might be due to the epigenetic modification particularly DNA hypomethylation through downregulation of DNMT1.

KEYWORDS
amarogentin, combination of drugs, DNMT1, EGCG, epigenetics, eugenol

1 | INTRODUCTION

Green tea polyphenol epigallocatechin gallate (EGCG) is a potent chemopreventive and chemotherapeutic agent as evident from several studies (Singh, Shankar, & Srivastava, 2011). It could modulate multiple cellular signaling and metabolic pathways including inhibition of cancer cell growth, invasion, metastasis, and induction of apoptosis in different experimental animal models as well as in cancer cell lines (Yang, Wang, Lu, & Picinich, 2009). EGCG could restrict the cell cycle at G1/S checkpoint through hypophosphorylation of retinoblastoma tumor suppressor protein (RB) and upregulation of P21, P16 along with downregulation of CYCLIND1 in different cancer cell lines and in vivo animal models (Liberto & Cobrinik, 2000; Manna, Mukherjee, Roy, Das, & Panda, 2009). The upregulation of P16 has been suggested to be due to its promoter demethylation as EGCG could inhibit the DNA methyltransferase activity in in vitro system (M. Fang, Chen, & Yang, 2007; M. Z. Fang et al., 2003). The hypophosphorylation of RB is regulated by different phosphatases, among them RBSP3 is important as it could dephosphorylate RB at Ser 807/811 at G1/S phase of cell cycle (Kashuba et al., 2009). In addition, another tumor suppressor gene LIMD1, has been shown to facilitate the RB-E2F interaction leading to the restriction of cell cycle at G1/S phase (Sharp et al., 2004). The inactivation of RBSP3 and LIMD1 has been seen in different carcinomas of oral, breast, and cervix as well as in mouse hepatocellular carcinoma (Ghosh et al., 2010; Mitra et al., 2010; Pal et al., 2012; Sinha et al., 2008). The association of EGCG in modulation of LIMD1 and RBSP3 expression has not yet been studied.

It has been seen that the chemopreventive–therapeutic potential of EGCG could be enhanced by combinatorial treatment of different antitumor antibiotic as well as natural compounds (Amin et al., 2010; Stearns & Wang, 2011). The synergistic action of EGCG:cisplatin and EGCG:doxorubicin was evident against growth of ovarian cancer cell line (Yunos, Beale, Yu, & Huq, 2011) and colony-forming ability of prostate cancer cell line, respectively (Stearns & Wang, 2011). Similarly, EGCG in combination with natural compounds like curcumin, luteolin, sapogenin, and so forth could synergistically inhibit the proliferative potential of different tumor cell lines (Amin et al., 2010; Oya et al., 2017; Jin et al., 2017; Khafif, Schantz, Chou, Edelstein, & Sacks, 1998). Thus, the combinatorial effect of EGCG with other natural compounds should be screened for better chemopreventive and therapeutic efficacies against tumor.

The cancer chemopreventive–therapeutic effect of eugenol (4-allyl-2-methoxyphenol), the active components of clove, has been seen in different in vitro and in vivo models (Cortés-Rojas, De Souza, & Oliveira, 2014; Khalil et al., 2017; Pal et al., 2010). Eugenol treatment could restrict the cell cycle at G1/S phase and induce apoptosis through downregulation of E2F, CYCLIND1, and upregulation of P21 in different in vitro studies (Al-Sharif, Remmal, & Aboussekhra, 2013; Junior et al., 2016). Similar result also observed in skin carcinogenesis mouse model (Pal et al., 2010). However, the effect of eugenol on retinoblastoma tumor suppressor protein (RB) phosphorylation and modulation of LIMD1 and RBSP3 during carcinogenesis has not yet been studied. Amarogentin, a secoiridoid glycoside is the active component of *Swertia Chirata*. The anticarcinogenic activity of this compound was first reported in a mouse skin and liver carcinogenesis model. In that study it was observed that amarogentin treatment restricted liver carcinogenesis at dysplastic stage due to upregulation of LIMD1, RBSP3, P16, and simultaneous downregulation of CYCLIND1 and hyperphosphorylated RB (Pal et al., 2012; Saha, Mandal, Das, Das, & Das, 2004). It could also induce apoptosis in liver cancer cells (Huang, Li, Zhang, & Gong, 2016).

Thus in this study, attempts have been made to understand the anticarcinogenic role of EGCG in combination with eugenol and amarogentin for better chemopreventive and therapeutic efficacies. For this study, the effect of EGCG, eugenol, and amarogentin individually and in combination on cell proliferation, apoptosis, and expression of some cell cycle regulatory genes like RB, ppRB, LIMD1, RBSP3, P16, and DNA methyltransferase 1 (DNMT1) were analyzed in a cervical cancer cell line Hela. Our data showed that EGCG–amarogentin combination had better antiproliferative and proapoptotic activity than EGCG–eugenol combination.

2 | MATERIALS AND METHODS

2.1 | Cell line and cell culture condition

Human cervical cancer cell line Hela obtained from National Centre for Cell Sciences, Pune, India. Mouse embryonic fibroblast (MEF) cell line was taken as normal cell line. This cell line was established in the laboratory from a 15-day-old Swiss MEFs (Mukherjee & Das, 1992). Both cell lines were maintained in minimal essential medium supplemented with 10% fetal bovine serum, 2 mM glutamine, 100 U penicillin, and 100 μg/ml of streptomycin. Cells were grown at 37°C in a humidified CO_2 incubator with 5% CO_2. Refeeding with fresh growth medium and subculturing (using 0.05% trypsin–EDTA) of cells was done as per requirement.

2.2 | Drugs used and preparation of drug stock solutions

EGCG (Sigma Chemical Co.) at 5 mg/ml in sterile water; eugenol (Sigma Chemical Co.) at 50 mg/ml in dimethyl sulfoxide (DMSO); amarogentin at 1 mg/ml in 10% ethanol water stock solutions were prepared as described previously (Manna et al., 2009; Pal et al., 2010).

2.3 | Cytotoxicity analysis

Cytotoxicity assay was performed with the sulforhodamine B (SRB) dye according to the standard protocol (Sur et al., 2016). Cells (5×10^3) were seeded into 96-well plates. After 24 hr cells were treated with different concentrations of EGCG (25–100 μg/ml), eugenol (25–350 μg/ml), and amarogentin (25–350 μg/ml) for 48 hr followed by fixation with 50% cold tricyclic antidepressant for 45 min at 4°C. The plate was then washed with distilled water and dried followed by treatment with SRB (0.4% wt/vol in acetic acid) for 10 min followed by washing with 1% acetic acid three times. Finally bound SRB was dissolved in 10 mM Trizma base. The optical density was measured at 540 nm using a microplate reader. As untreated solvent control, the cells were treated with corresponding solvents (eugenol: DMSO; amarogentin: 10% ethanol). The cell growth inhibition was plotted against different drug doses. The cell inhibition due to only solvent was deducted from cell inhibition after drug (dissolved in corresponding solvent) treatment to get the actual effect of drug. Inhibitory concentration 50% (IC_{50}) was calculated using a logarithmic plot as described by Khafif et al. (1998). The graphs were plotted between log(*D*) versus log(f_a/f_u). Log(*D*): log value of doses of drugs; log(f_a/f_u): log of the ratio of cellular fraction affected (f_a) and fraction unaffected (f_u) by drug treatment.

The combination index (CI) determined by using Chou–Talalay method (Chou, 2010). The CI values <0.9: synergistic; values 0.9–1.1: additive, and values >1.1: antagonistic were considered for the effect of combinations of two compounds as described by Chou (2010).

The dose-reduction index (DRI) is a measure of dose reduction of each drug in a synergistic combination at a given effect level, compared with the doses of each drug alone calculated according to using Chou–Talalay method (Chou, 2010).

2.4 | Anchorage-independent growth assay

This assay was carried out over soft agar (low melting point [LMP] agarose) according to standard procedure (Borowicz et al., 2014). Here cell suspension (20,000 cells) was mixed with top layer LMP agarose (0.4%) and spread over already solidified base layer LMP

agarose (0.8%) in six-well plates. Cells were treated with drugs (at respective IC_{50} value) individually and in combinations after 24 hr of cell seeding. Cells were allowed to grow for 20 days with change in media every 3 days interval and regularly monitored for colony formation. After that cells were fixed and stained with 0.1% crystal violet in 10% ethanol for 30 min followed by washing excess dye. Cells were then observed and photographed under a microscope (Olympus ckzx 41, Tokyo, Japan). Colony size and numbers were calculated under microscope and plotted against different experimental groups and compared.

2.5 | Apoptosis analysis

Detection of apoptotic cells was assessed by the terminal deoxynucleotidyl transferase dUTP nick-end labeling (TUNEL) method using in situ cell death detection kit (Roche Molecular Biochemicals, Manheim, Germany) according to standard procedure (Pal et al., 2012). Cells (20,000 cells per cover slip) were grown and incubated without or with drugs (at respective IC_{50} dose) for 48 hr. The cells were fixed with 4% paraformaldehyde, and permeabilized with 0.1% Triton X-100 in 0.1% sodium citrate. After washing, cells were incubated with the TUNEL reaction mixture for 60 min at 37°C. The stained cells were then analyzed with a fluorescence microscope (Leica DM 4000 B; Wetzlar, Germany) at ×40 magnification and photographed. Apoptosis positive cell percentage for each experimental group is plotted graphically and compared.

2.6 | Expression analysis

2.6.1 | mRNA expression analysis

Total RNA was extracted from cells (1×10^6 per 100 mm) without or with drugs (at respective IC_{50} dose) treatment individually and in combinations and incubated for 48 hr using TRIzol reagent according to the manufacturer's protocol (Pal et al., 2012). cDNA was synthesized from the 10 mg of total RNA with superscript III reverse transcriptase (Life Technologies, Carlsbad, CA) according to manufacturer's protocol (Pal et al., 2012). Gene expression was carried out with power SYBR Green PCR Master Mix (Life Technologies, Carlsbad, CA) in real-time PCR (Roche) using specific primers (Supporting Information document). Relative gene expression data were analyzed using the $2^{-\Delta\Delta Ct}$ method (Livak et al., 2002). Relative expression analysis was performed in three replicates. Human β2-microglobulin gene (B2M) was used as endogenous control. Relative expression was graphically represented.

2.6.2 | Protein extraction and western blot analysis

Protein was extracted from cells (1×10^6 per 100 mm) without or with drugs (at respective IC_{50} dose) treatment individually and in combinations for 48 hr. Cell lysate was prepared from both control and treated cells by sonication with RIPA buffer (25 mM Tris–HCl [pH 7.6], 150 mM NaCl, 0.1% Triton X-100, 1 mM EDTA, 0.1% sodium dodecyl sulfate [SDS], 1% sodium deoxycholate, 1 μg/ml aprotinin, 1 μg/ml leupeptin, 1 mM PMSF, 10 mM NaF, and 1 mM sodium orthovanadate). Equal amount of proteins were separated by 10–12% SDS–PAGE and then transferred to polyvinylidine difluoride (PVDF) membrane (Millipore, MA, USA). Membranes were incubated with 3–5% nonfat drymilk for 1–2 hr at room temperature followed by overnight incubation at 4ºC with desired primary antibodies (Supporting Information document; 1:500–1:1,000 in 1% nonfat dry milk) and corresponding HRP-conjugated secondary antibodies (Supporting Information document; 1:2,000–1:10,000 in 1% nonfat dry milk) for 2 hr at room temperature (Pal et al., 2012). The protein bands were then visualized using luminol reagent and autoradiographed on X-ray film (Kodak, Rochester, NY). All the immunoblotting experiments were performed in three replicates. The band intensities were quantified using densitometric scanner (BioRad GS-800; BioRad, Hercules, CA). Peak densities of the proteins of interest were normalized using peak density of loading control α-tubulin.

2.6.3 | Immunocytochemical analysis

Monolayer cells (20,000 cells per cover slip) were grown on sterile cover slip for 24 hr. Cells were treated without or with drugs (at respective IC_{50} dose) individually and in combinations for 48 hr. Cover slips were fixed with methanol at −20°C. Before staining cover slips were rehydrated and washed with phosphate buffer saline (PBS) for 30 min. Endogenous peroxidase was blocked by 0.3% H_2O_2 in 1× PBS for 5–10 min. Cells were then permeabilized with 0.1% Triton X for 15 min. The nonspecific binding sites were blocked by 3–5% bovine serum albumin (BSA) for 1–2 hr followed by overnight incubation with primary antibodies (Supporting Information document; 1:80–1:100 in 1% BSA) and fluorescein isothiocyanate–conjugated secondary antibody (Supporting Information document; 1:500 in 1% BSA) for 1 hr. Cells were then treated with nuclear staining dye 4′,6-diamidino-2-phenylindole (1 μg/ml) for 1 min and washed repeatedly (Sur et al., 2016). Finally cover slips were glycerol mounted on clean glass slides and photographed using fluorescense microscope (Leica DM 4000 B; Leica, Germany).

2.7 | Methylation analysis

High-molecular-weight DNA was extracted according to standard procedure (Dasgupta et al., 2002) from cells (1×10^6 cells per 100 mm plate) treated without or with drugs (at respective IC_{50} value) individually and in combinations for 48 hr. After treatment cells were harvested with trypsinization and DNA was extracted by proteinase-K digestion, followed by phenol–chloroform extraction method (Dasgupta et al., 2002). The promoter methylation status of LIMD1, RBSP3, and P16 were analyzed by PCR-based methylation-sensitive restriction analysis (MSRA) method using methylation-sensitive HpaII enzyme (Roche Diagnostics, Mannheim, Germany) and specific primers (Supporting Information document; Mitra et al., 2010). Approximately 100 ng of DNA samples were individually digested overnight with HpaII. β-*3A-ADAPTIN* gene (K1; 445 base

pairs, bp) and fragment of *RAR* β2 exon-1 (K2; 229 bp) were used as digestion and integrity controls, respectively (Loginov et al., 2004). Mock digestion was done with each sample without any restriction enzymes. PCR products were analyzed on 2% agarose gel, visualized under gel documentation system (BioRad, GS-800; Philadelphia, PA) and photographed.

2.8 | Statistical analysis

Results are expressed as mean ± *SD*. Differences between groups were determined by χ^2 trends. $p < 0.05$ and <0.001 were considered as statistically significant. Treated groups were compared with control group.

3 | RESULTS

3.1 | Inhibition of cellular proliferation by EGCG, eugenol, and amarogentin individually and in combination

Treatment with individual compounds inhibited Hela cell growth in dose-dependent manner (Figure 1a). EGCG is the most effective

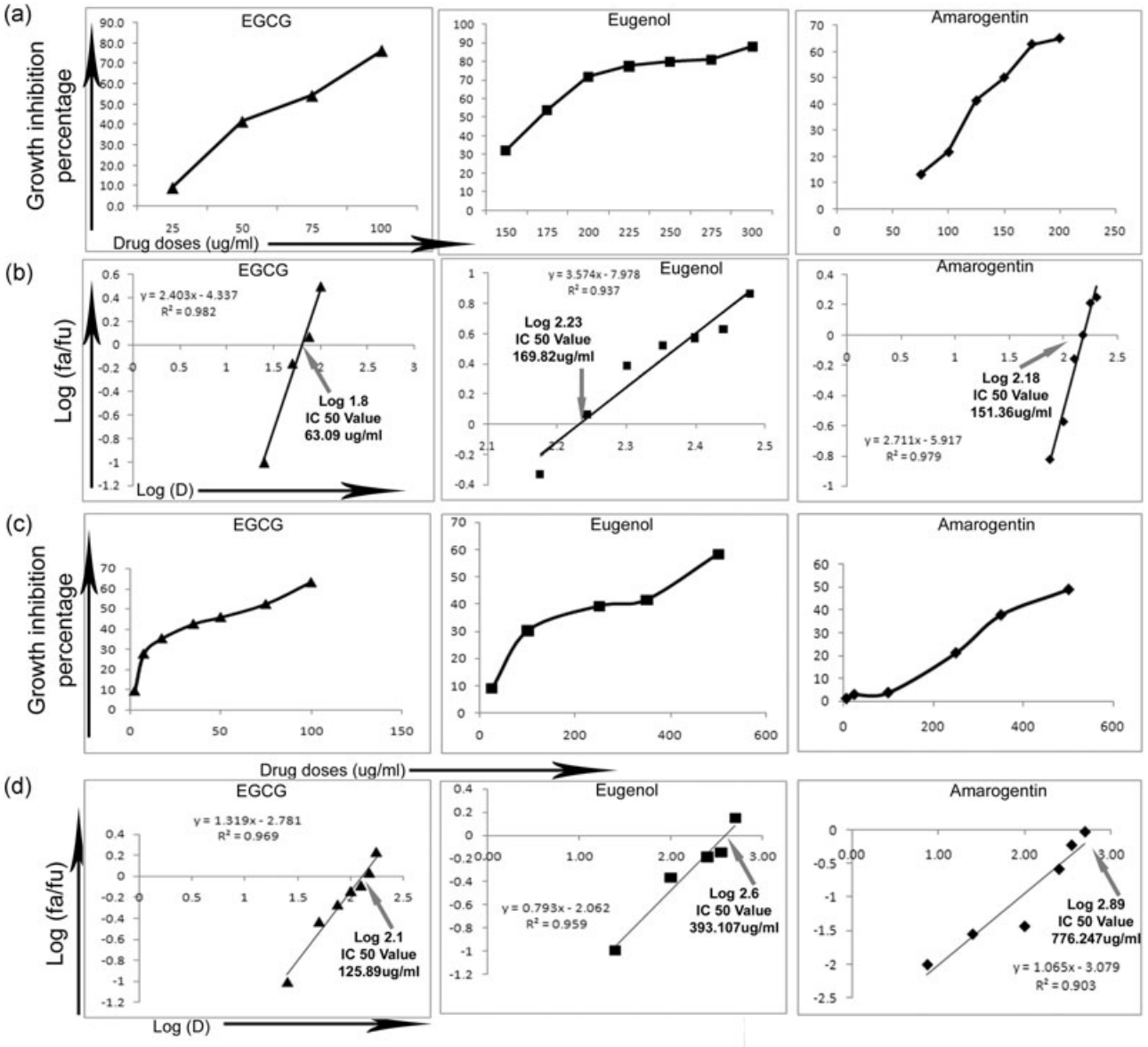

FIGURE 1 (a) Cell growth inhibition percentage is plotted against increasing drug doses (μg/ml) of EGCG, eugenol, and amarogentin in Hela cells, respectively. (b) IC_{50} values of EGCG, eugenol, and amarogentin were determined from the log plot. Corresponding IC_{50} values were mentioned in these graphs with gray arrows. (c) Cell growth inhibition percentage is plotted against increasing drug doses (μg/ml) of EGCG, eugenol, and amarogentin in normal MEF cells, respectively. (d) IC_{50} values of EGCG, eugenol, and amarogentin against normal mouse embryonic fibroblast cells were determined from the log plot. Corresponding IC_{50} values were mentioned in these graphs with gray arrows. EGCG: epigallocatechin gallate; IC: inhibitory concentration; MEF: mouse embryonic fibroblast

(IC_{50}: 63.09 μg/ml) followed by amarogentin (IC_{50}: 151.36 μg/ml) and eugenol (IC_{50}: 169.82 μg/ml; Figure 1a,b). On the other hand, the drugs are not so much effective on normal MEF cell line with much higher IC_{50} values (EGCG IC_{50}: 125 μg/ml; eugenol IC_{50}: 393 μg/ml; IC_{50}: 776 μg/ml amarogentin) than Hela cells (Figure 1c,d).

In different combinatorial analysis of the drugs on Hela cell growth it was evident that EGCG (7.5 μg/ml) in combination with eugenol (114.8 μg/ml) or EGCG (10 μg/ml) in combination with eugenol (95.5 μg/ml) inhibited 50% of the cell growth synergistically (Figure 2a,b; Supporting Information Table). Similarly EGCG (7.5 μg/ml) in combination with amarogentin (97.95 μg/ml) or EGCG (10 μg/ml) in combination with amarogentin (87.1 μg/ml) inhibited 50% of the cell growth synergistically (Figure 2a,b; Supporting Information Table). For further experiment the combination which showed lower CI value were selected (Supporting Information document), that is, EGCG 10 μg/ml combined with 95.5 μg/ml eugenol (C1) and 87.1 μg/ml amarogentin (C2). The dose reduction indexes (DRI) for EGCG (6.3) followed by eugenol (1.78) and amarogentin (1.74) (Supporting Information Table). Thus, low concentrations of the drugs in combination could effectively inhibit the cell growth.

Significant change in cell density and cellular morphology were observed after treatment with the drugs either alone or in combination at corresponding IC_{50} values (Figure 2c).

3.2 | Effect on anchorage-independent growth due to the treatment of EGCG, eugenol, and amarogentin individually and in combination

It was evident that, these drugs individually and in both combinations can affect the colony formation efficiency of cancer cells (Figure 3). The number of average colonies (±35) formed in the control cells were not changed considerably in individually treated groups (~30–28). However, significant reduction in colony formation was evident in case of combinatorial treatment (~20–18; Figure 3a,b). On the other hand, the sizes (>20 μM) of the colonies significantly reduced in case of individual treatment as well as in combination (Figure 3a,c). Thus, the drugs in combination could highly reduce the colony formation ability.

3.3 | Induction of apoptosis by EGCG, eugenol, and amarogentin individually and in combination

The Hela cells showed differential apoptotic index after individual treatment of the drugs or in combination. The apoptotic index was significantly increased after treatment with amarogentin and in both combinations C1 and C2 (Figure 4a,b). Similar trend has also been seen in analysis of activated caspase-3 expression (Figure 4c,d). Antiapoptotic protein BCL2 expression also found to be downregulated in treated

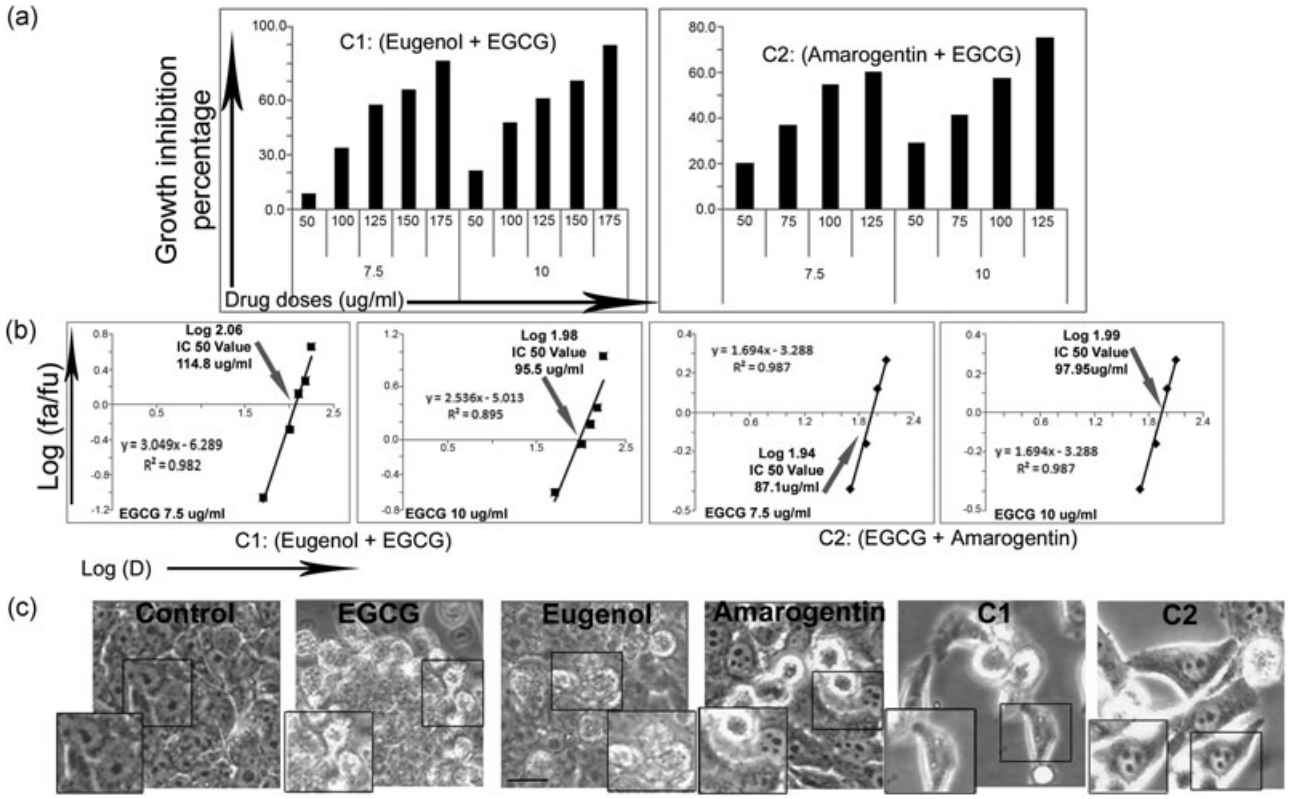

FIGURE 2 (a) Histograms are plotted against cell growth inhibition percentage versus two concentrations (μg/ml) of EGCG with five concentrations of eugenol (C1) and two concentrations (μg/ml) of EGCG with four concentrations of amarogentin (C2). (b) IC_{50} values are determined (marked with gray arrows) from corresponding log plots of each combination. (e) Cellular morphology after treatment with the drugs individually and in combinations. Magnifications ×40. Scale bar = 50 mm. Part of these figures are enlarged and given in inset for better understanding the cellular morphology. EGCG: epigallocatechin gallate; IC: inhibitory concentration

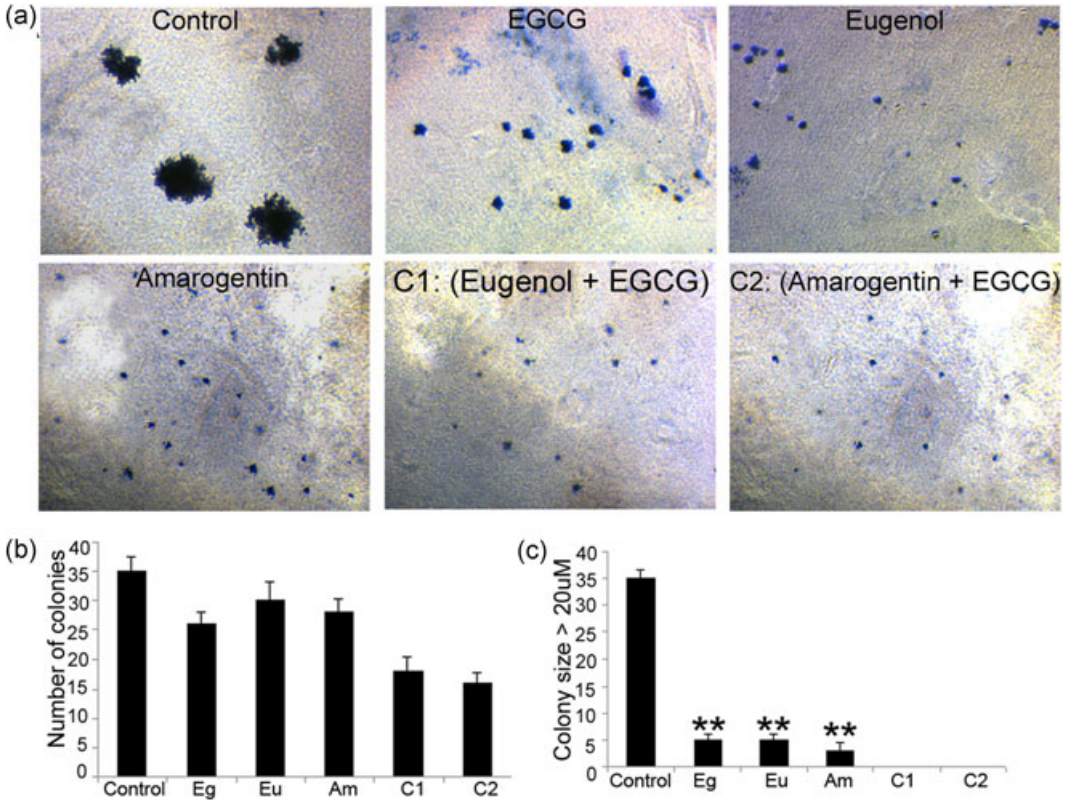

FIGURE 3 (a) Representative images of soft agar colonies of different experimental groups. Histograms are shown to represent (b) total number of colonies in each group and (c) numbers of colonies with sizes (>20 μM) in each group; $^{**}p < 0.01$ [Color figure can be viewed at wileyonlinelibrary.com]

cells than control (Figure 4c,d). In case of combined treatment its expression was further downregulated (Figure 4c,d).

3.4 | Effect of EGCG, eugenol, and amarogentin individually and in combination on key regulatory genes in the G1/S phase of cell cycle

In quantitative mRNA and western blot analysis, RB did not change significantly after individual treatment of the drugs and also in combination (Figure 5a–c). However, ppRB (Ser 807/811) protein expression significantly decreased after individual treatment of the drugs (except eugenol) and also in combination (Figure 5b). Similar trend has also been seen in case of ppRB (Ser 567) protein expression (Figure 5b).

In immunocytochemical analysis, Rb expression was seen mainly in the cytoplasm whereas, ppRB (Ser 807/811) and ppRB (Ser 567) expressions were seen in both nucleus and cytoplasm (Figure 5d). In case of EGCG and amarogentin treatment increased the RB expression in the nucleus with considerable reduced expression of both ppRBs (Figure 5d). On the other hand, eugenol treatment reduced the nuclear expression of ppRBs slightly without changes in the pattern of RB expression (Figure 5d). In combinatorial treatment (C1 and C2), the expression of both ppRB was highly reduced without changes in RB expression (Figure 5d). This indicates the inhibition of RB phosphorylation by the drugs either alone or in combinations.

To understand the mechanism of inhibition of RB phosphorylation the expression (mRNA/protein) of G1/S cell cycle inhibitors LIMD1, RBSP3, and P16 along with activator CYCLIND1 were analyzed. The mRNA expression of LIMD1, RBSP3, and P16 increased after drug treatment and significant increase was observed in case of C1 and C2 (Figure 6a–c). Similar trend has been seen in case of protein expression (Figure 6a–c). On the other hand, mRNA and protein expression of CYCLIND1 was decreased after individual and combined treatment of the drugs with significant decrease in EGCG, amarogentin, and combined treatment (Figure 6a–c).

In immunocytochemical analysis considerable increase in cytoplasmic expression of LIMD1 has been seen after treatment with drugs either alone or in combination (Figure 6d). Similarly, cytoplasmic and nuclear expressions of RBSP3 and P16 have been increased after treatment with drugs either alone or in combination. However, the expression increased more in combination (Figure 6d).

Thus, the increased expression of LIMD1, RBSP3 and P16 along with reduced expression of CYCLIND1 could synergistically reduce the Rb phosphorylation after treatment of the drugs either alone or in combination resulting G1/S cell cycle blockage.

3.5 | Effect of EGCG, eugenol, and amarogentin individually and in combination on epigenetic modification of the regulators of cell cycle

To understand the mechanism of upregulation of the cell cycle inhibitors LIMD1, RBSP3, and P16 after treatment of drugs promoter methylation status of these genes were analyzed. Hypomethylation

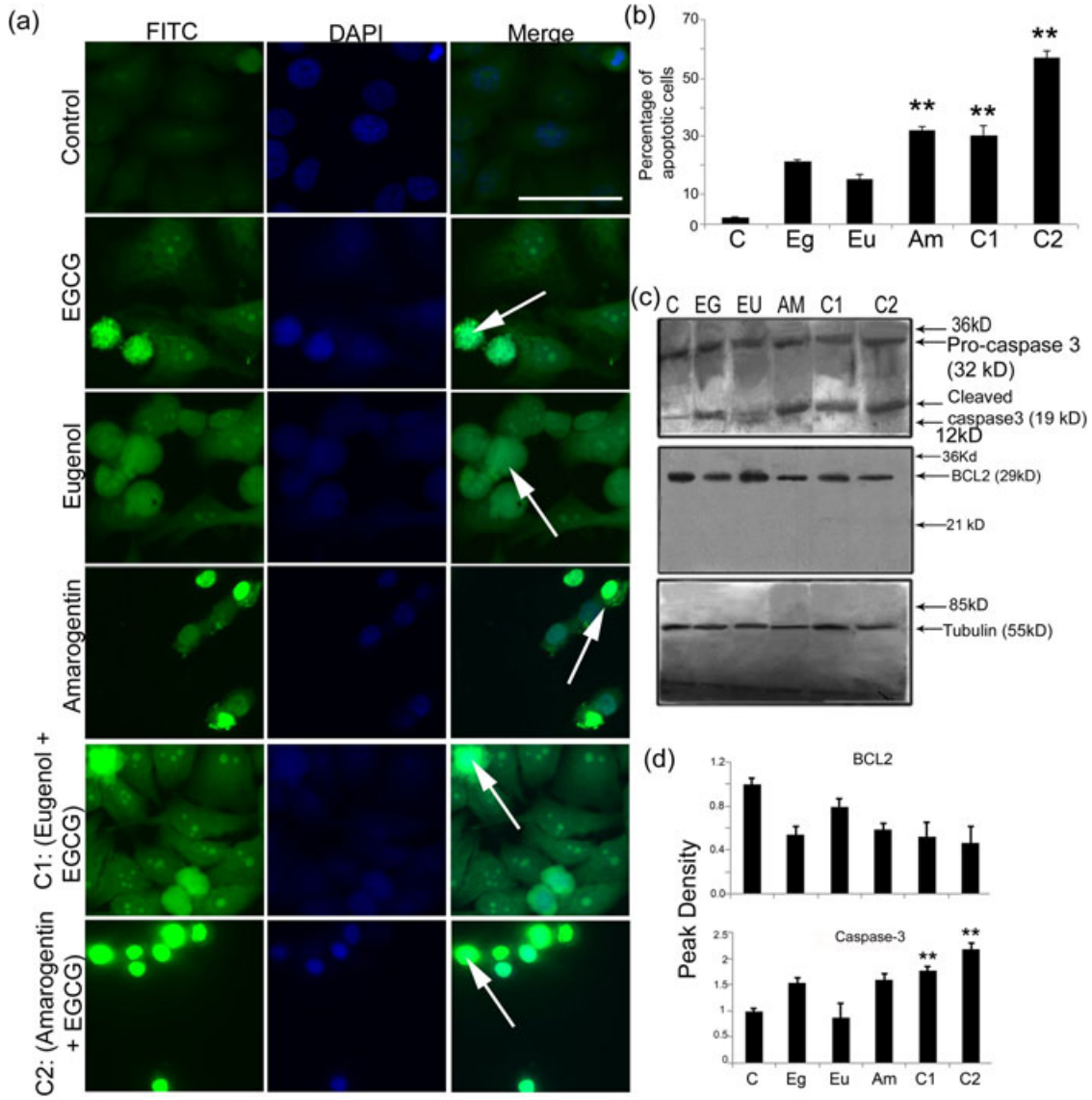

FIGURE 4 (a) Representative images of apoptotic cells in different experimental groups. Here TUNEL positive cells were marked with white arrows. (b) Histograms are shown for percentage of apoptotic cells for each experimental group; $^{**}p < 0.01$. (c) Western blot analysis showing expression of procaspase-3, cleaved caspase-3, and BCL2 with loading control tubulin. (d) Normalized peak densities of protein expression of BCL2 and cleaved caspase-3 are plotted against each experimental group control (C), EGCG (EG), eugenol (EU), and amarogentin (AM), EGCG:eugenol combination (C1), and EGCG:amarogentin (C2). Molecular weight marker points are marked along the side of the autoradiographs. EGCG: epigallocatechin gallate; TUNEL: transferase dUTP nick-end labeling [Color figure can be viewed at wileyonlinelibrary.com]

of the promoters of LIMD1 and P16 has been seen after treatment of drugs alone or in combination (Figure 7b). No such changes have been seen in case of RBSP3 after treatment of the drugs (Figure 7b).

3.6 | Effect of EGCG, eugenol, and amarogentin individually and in combination on expression of DNMT1

To understand the mechanism of hypomethylation of the promoter region of LIMD1 and P16, the expression of DNMT1 was analyzed. The mRNA expression of DNMT1 significantly decreased after treatment of the drugs either alone or in combination (Figure 8a). The combinatorial treatment of the drugs has been seen to be more effective than individual treatment (Figure 8a). The immunocytochemical analysis showed reduced nuclear expression of DNMT1 in the treated cells and combined treatment further downregulated the expression of DNMT1 (Figure 8b).

4 | DISCUSSION

In this study the chemotherapeutic efficacies of EGCG, eugenol, and amarogentin either individually or EGCG in combination with eugenol–amarogentin were evaluated in Hela cell line. The compounds were seen to be much more sensitive to the Hela cell line than normal MEF, indicating their chemotherapeutic efficacies

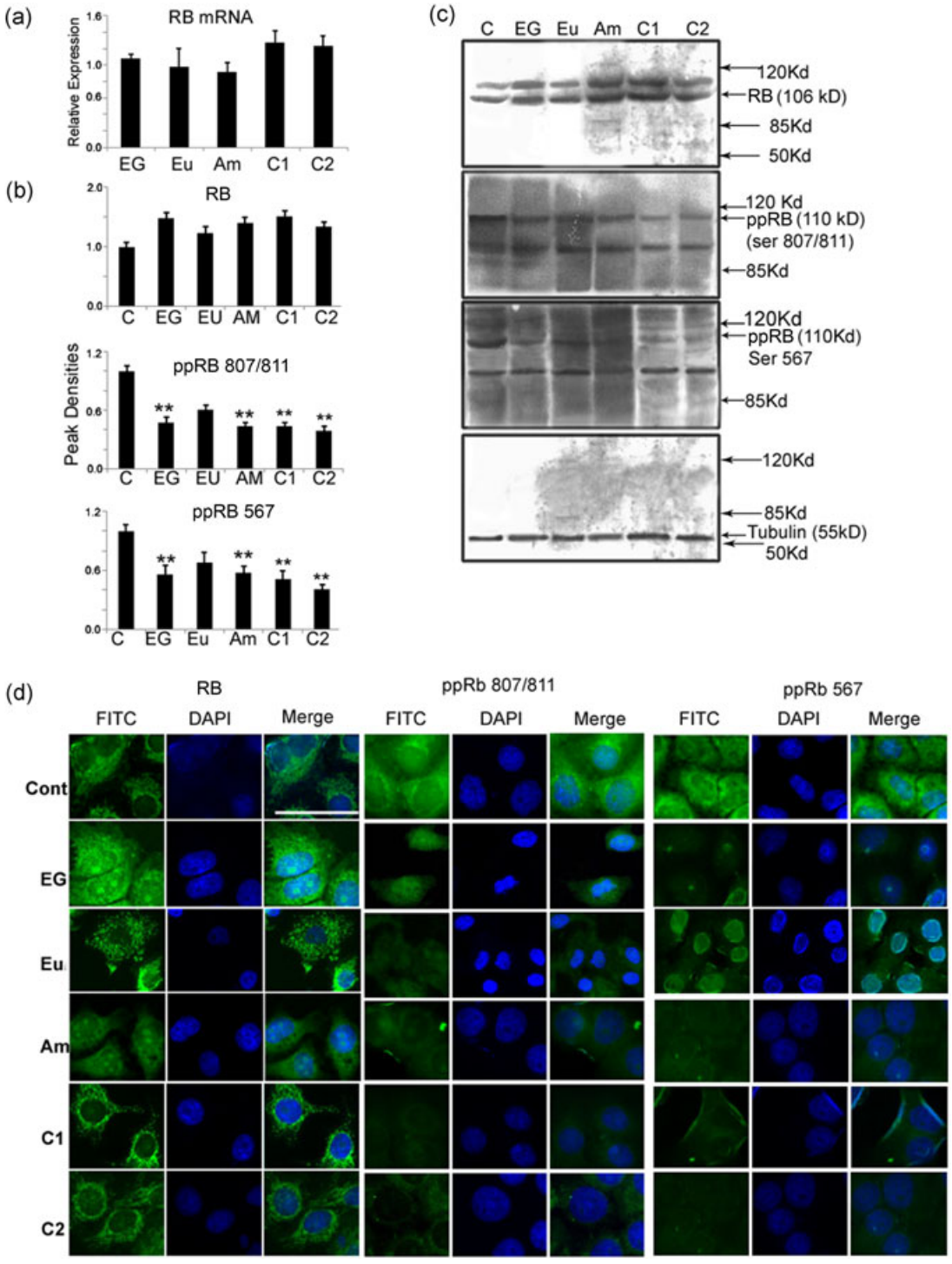

FIGURE 5 Expression analysis of whole RB, ppRB (Ser 807/811), and ppRB (Ser 567). (a) mRNA analysis of whole RB. (b) Histograms showing quantitative analysis of normalized peak densities of the above proteins for each experimental group control (C), EGCG (EG), eugenol (EU), amarogentin (AM), EGCG:eugenol combination (C1), and EGCG:amarogentin (C2); $^{**}p < 0.01$. (c) Western blot analysis showing expression of RB, ppRB (Ser 807/811), and ppRB (Ser 567). Molecular weight marker points are marked along the side of the autoradiographs. (d) Immunocytochemical expression analysis of RB, ppRB Ser 807/811, and ppRB Ser 567. Magnifications ×40. Scale bar = 50 mm. mRNA: messenger RNA; EGCG: epigallocatechin gallate [Color figure can be viewed at wileyonlinelibrary.com]

(Figure 1). Among these compounds EGCG was most effective (Figure 1). The antiproliferative and proapoptotic activity of EGCG was found against several cancer cell lines excluding normal human fibroblast cell line (Luo, Luo, & Yu, 2010; Tao, Park, & Lambert, 2015; Weisburg, Weissman, Sedaghat, & Babich, 2004). Chemotherapeutic potential of eugenol was reported against different cancer cell line (Jaganathan & Supriyanto, 2012). Anticancer effect of amarogentin was reported against liver cancer cell line (Sur et al., 2016). However,

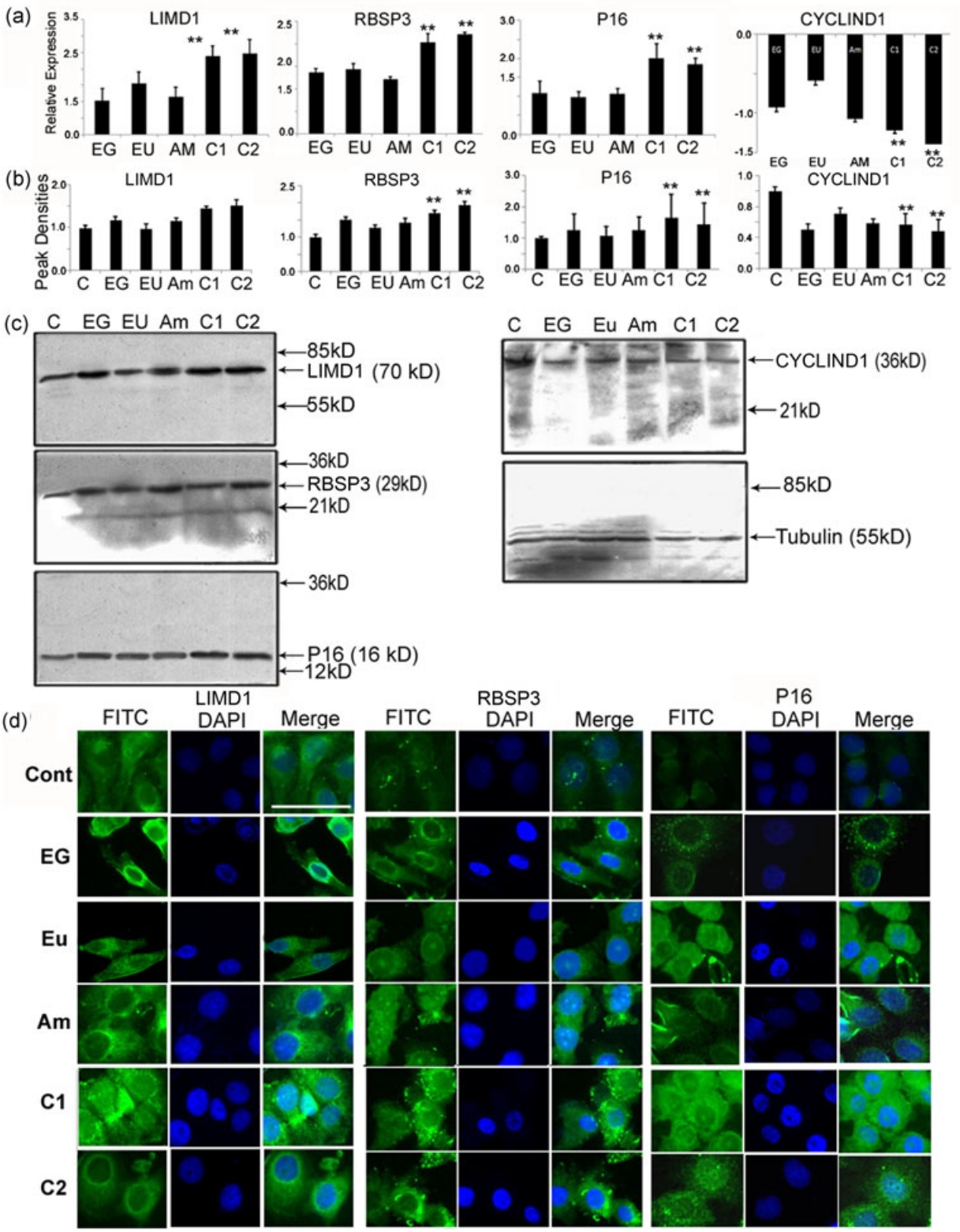

FIGURE 6 Expression analysis of LIMD1, RBSP3, P16 and CYCLIND1. (a) mRNA analysis of the above genes. (b) Histograms showing quantitative analysis of normalized peak densities of the above proteins for each experimental group control (C), EGCG (EG), eugenol (EU), amarogentin (AM), EGCG:eugenol combination (C1), and EGCG:amarogentin (C2); $^{**}p < 0.01$. (c) Western blot analysis showing expression of corresponding proteins. Scale bar = 50 mm. Molecular weight marker points are marked along the side of the autoradiographs. (d) Immunocytochemical expression analysis of LIMD1, RBSP3 and P16. Magnifications ×40. mRNA: messenger RNA; EGCG: epigallocatechin gallate [Color figure can be viewed at wileyonlinelibrary.com]

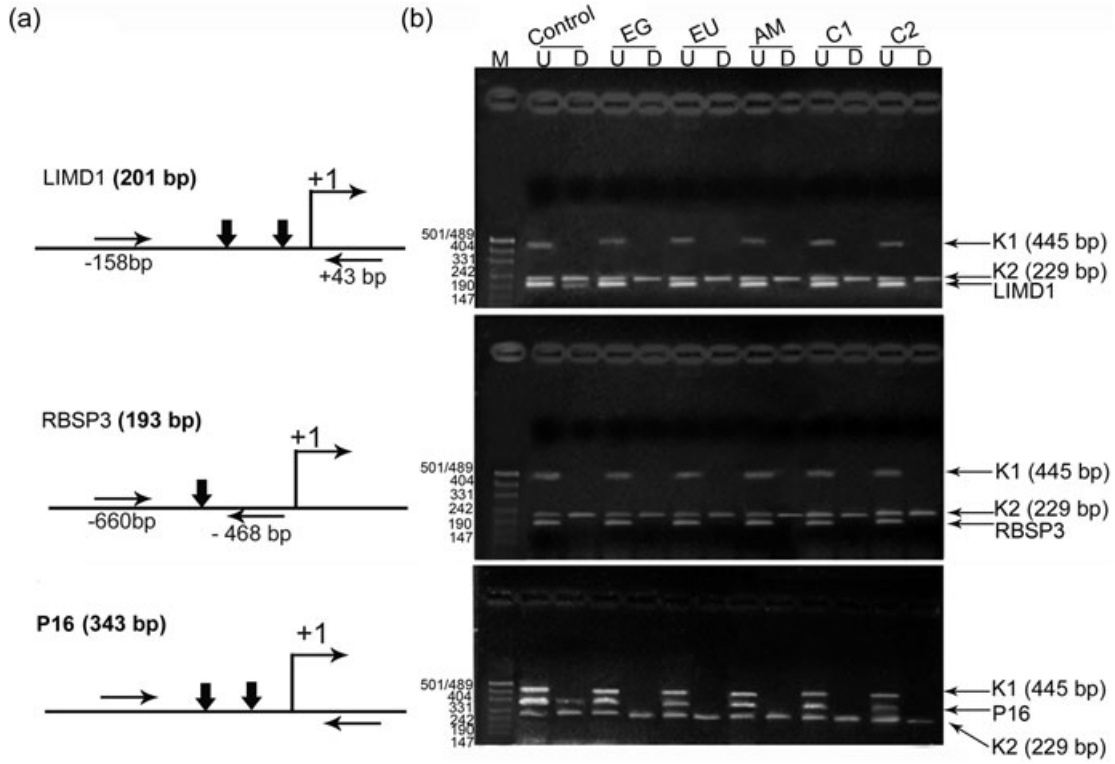

FIGURE 7 Methylation analysis of LIMD1, RBSP3 and P16. (a) Schematic diagram showing promoter region including primer position (horizontal arrows), numbers of restriction site (down arrows), and transcription start site (+1). (b) Corresponding gel images showing band patterns of undigested (U) and digested (D) samples of each group, control (C), EGCG (EG), eugenol (EU), amarogentin (AM), EGCG:eugenol combination (C1), and EGCG:amarogentin (C2). pUC 19 plasmid Msp1 digested is loaded as marker (M) in the left most lane, band sizes are mentioned. EGCG: epigallocatechin gallate

effects of eugenol and amarogentin against normal cell line were not reported earlier. In combination treatment, EGCG along with eugenol–amarogentin could inhibit the tumor cell proliferation at low concentrations, indicating the effectiveness of this treatment than individual compound (Figure 2, Supporting Information Table). Combined treatment of EGCG and different other natural compounds like luteolin and sapogenin also found to enhance the cancer cell growth inhibition and apoptosis rate (Amin et al., 2010; Du et al., 2013).

It was evident that the combinatorial treatments could reduce the colony formation abilities of Hela cell line than individual treatment, indicating its better antitumor efficacy (Figure 2). It has been shown that EGCG along with doxorubicin inhibited the colony-forming ability of prostate cancer cells synergistically (Stearns & Wang, 2011). It seems that better antitumor efficacies of combinatorial treatment might be due to enhanced apoptosis rate than individual treatment as seen in our study (Figure 4). Interestingly, EGCG–amarogentin combination showed higher apoptotic percentage than EGCG–eugenol. This has been validated by cleaved caspase-3 expression (Figure 4). It was evident that EGCG with other natural compounds synergistically induced increased apoptosis than individual compound (Amin et al., 2010; Oya et al., 2017).

It was evident that the combinatorial treatment could highly modulate the genes associated with G1/S cell cycle checkpoint than individual treatment. The phosphorylation of RB at Ser 807/811 and Ser 567 was seen to be highly reduced due to combinatorial treatment than individual. This might be due to the increased expression of LIMD1, RBSP3 and P16 along with reduced expression of cyclinD1 in the combinatorial treatment. This suggests that the combinatorial treatment could effectively block the cell cycle at G1/S cell cycle checkpoint of the Hela cell line resulting induction of apoptosis. It was evident that EGCG treatment increased the cell percentage at subG0 phase and restricted cells at G1/S phase of cell cycle (Luo et al., 2010). Similarly, eugenol treatment increased the percentage of cells in subG0 phase and G1/S phase indicating the apoptotic cell death and restriction of cell cycle at this phase and abrogation of G2/M phase in different cancer cell lines (Junior et al., 2016). Indication of G1/S phase restriction was evident in case of amarogentin treatment by upregulation of P16, LimD1, Rbsp3 and downregulation of ppRbs in liver cancer mouse model (Pal et al., 2012). Thus, it seems that in both combinations the growth of the cells will be restricted at G1/S phase of cell cycle.

The upregulation of LIMD1 and P16 in the Hela cell line after treatment with individual as well as combination of two compounds have been suggested to be due to hypomethylation of their promoter regions as seen in the methylation analysis (Figure 7). The expression of LIMD1, P16, and RBSP3 was further increased due to combined treatment indicating their synergistic action of the compounds.

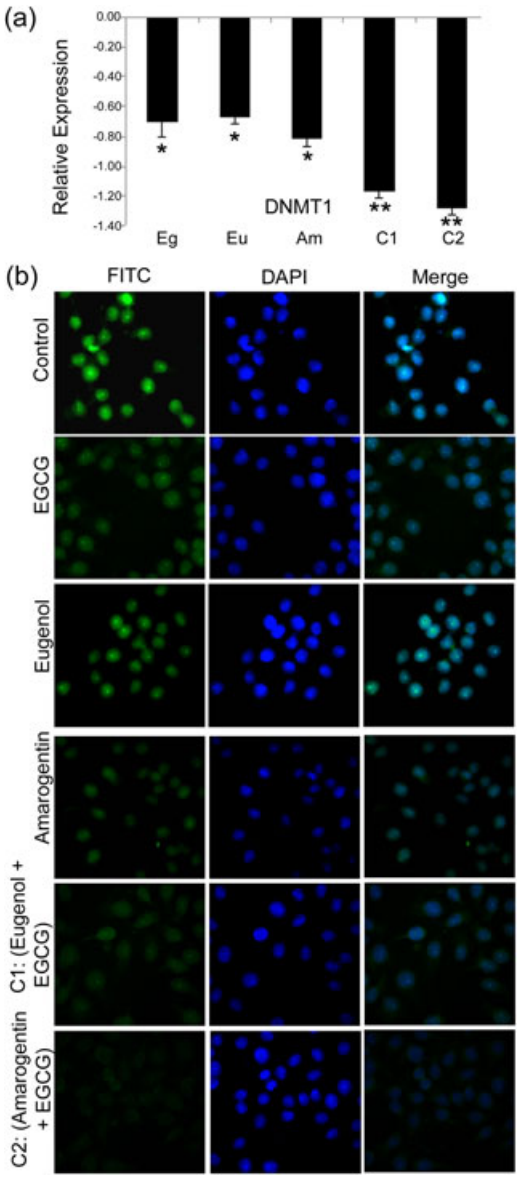

FIGURE 8 Expression analysis of DNMT1. (a) mRNA analysis; *$p < 0.05$ and **$p < 0.01$. (b) Immunocytochemical expression analysis of DNMT1. Magnifications ×40. Scale bar = 50 mm. mRNA: messenger RNA; DNMT1: DNA methyltransferase 1 [Color figure can be viewed at wileyonlinelibrary.com]

However, no promoter hypomethylation of RBSP3 was seen in Hela cell line. So, upregulation of this gene might be due to hypomethylation of other regulatory regions or by some other means. It seems that the hypomethylation of LIMD1 and P16 might be due to the downregulation of DNMT1 (Figure 8). The reduced expression of DNMT1 by EGCG has been reported by different studies (Henning, Wang, Carpenter, & Heber, 2013; Morris et al., 2016), but no such phenomenon has been reported in case eugenol and amarogentin.

In this study, it seems that apart from affecting common pathways by the drugs to restrict cellular proliferation and induction of apoptosis, the drugs could also inhibit different cellular pathways simultaneously to inhibit the cellular processes. As a result synergistic action of the drugs has been seen.

ACKNOWLEDGMENTS

Authors are grateful to the Director, Chittaranjan National Cancer Institute, Kolkata, for his kind support for the work. Financial support for this study was provided by grant 09/030(0074)/2014 EMR-I from CSIR, New Delhi to D. P.

CONFLICTS OF INTEREST

The authors declare that there are no conflicts of interest.

ORCID

Chinmay Kumar Panda http://orcid.org/0000-0002-0854-6978

REFERENCES

Al-Sharif, I., Remmal, A., & Aboussekhra, A. (2013). Eugenol triggers apoptosis in breast cancer cells through E2F1/survivin down-regulation. *BMC Cancer*, *13*, 600.

Amin, A. R., Wang, D., Zhang, H., Peng, S., Shin, H. J., Brandes, J. C., … Shin, D. M. (2010). Enhanced anti-tumor activity by the combination of the natural compounds (-)-epigallocatechin-3-gallate and luteolin: Potential role of p53. *Journal of Biological Chemistry*, *285*, 34557–34565.

Borowicz, S., Van Scoyk, M., Avasarala, S., Karuppusamy Rathinam, M. K., Tauler, J., Bikkavilli, R. K., & Winn, R. A. (2014). The soft agar colony formation assay. *Journal of Visualized Experiments*, *92*, e51998.

Chou, T. C. (2010). Drug combination studies and their synergy quantification using the Chou–Talalay method. *Cancer Research*, *70*, 440–446.

Cortés-Rojas, D. F., De Souza, C. R. F., & Oliveira, W. P. (2014). Clove (*Syzygium aromaticum*): A precious spice. *Asian Pacific Journal of Tropical Biomedicine*, *4*, 90–96.

Dasgupta, S., Mukherjee, N., Roy, S., Roy, A., Sengupta, A., Roychowdhury, S., & Panda, C. K. (2002). Mapping of the candidate tumor suppressor genes' loci on human chromosome 3 in head and neck squamous cell carcinoma of an Indian patient population. *Oral Oncology*, *38*(1), 6–15.

Du, G. J., Wang, C. Z., Qi, L. W., Zhang, Z. Y., Calway, T., He, T. C., … Yuan, C. S. (2013). The synergistic apoptotic interaction of panaxadiol and epigallocatechin gallate in human colorectal cancer cells. *Phytotherapy Research*, *27*, 272–277.

Fang, M., Chen, D., & Yang, C. S. (2007). Dietary polyphenols may affect DNA methylation. *Journal of Nutrition*, *137*, 223S–228S.

Fang, M. Z., Wang, Y., Ai, N., Hou, Z., Sun, Y., Lu, H., … Yang, C. S. (2003). Tea polyphenol (-)-epigallocatechin-3-gallate inhibits DNA methyltransferase and reactivates methylation-silenced genes in cancer cell lines. *Cancer Research*, *63*, 7563–7570.

Ghosh, S., Ghosh, A., Maiti, G. P., Mukherjee, N., Dutta, S., Roy, A., … Panda C. K. (2010). LIMD1 is more frequently altered than RB1 in head and neck squamous cell carcinoma: Clinical and prognostic implications. *Molecular Cancer*, *9*, 58.

Henning, S. M., Wang, P., Carpenter, C. L., & Heber, D. (2013). Epigenetic effects of green tea polyphenols in cancer. *Epigenomics*, *5*, 729–741.

Huang, C., Li, R., Zhang, Y., & Gong, J. (2016). Amarogentin induces apoptosis of liver cancer cells via upregulation of p53 and down-regulation of human telomerase reverse transcriptase in mice. *Technology in Cancer Research & Treatment*, *16*, 546–558.

Jaganathan, S. K., & Supriyanto, E. (2012). Antiproliferative and molecular mechanism of eugenol-induced apoptosis in cancer cells. *Molecules*, *17*, 6290–6304.

Jin, G., Yang, Y., Liu, K., Zhao, J., Chen, X., Liu, H., … Dong, Z. (2017). Combination curcumin and (-)-epigallocatechin-3-gallate inhibits colorectal carcinoma microenvironment-induced angiogenesis by JAK/STAT3/IL-8 pathway. *Oncogenesis*, *6*, e384.

Júnior, P. L., Câmara, D. A., Costa, A. S., Ruiz, J. L., Levy, D., Azevedo, R. A., … Ferreira, A. K. (2016). Apoptotic effect of eugenol envolves G2/M phase abrogation accompanied by mitochondrial damage and clastogenic effect on cancer cell in vitro. *Phytomedicine*, *23*, 725–735.

Kashuba, V. I., Pavlova, T. V., Grigorieva, E. V., Kutsenko, A., Yenamandra, S. P., Li, J., … Zabarovsky, E. R. (2009). High mutability of the tumor suppressor genes RASSF1 and RBSP3 (CTDSPL) in cancer. *PLoS One*, *4*, e5231.

Khafif, A., Schantz, S. P., Chou, T. C., Edelstein, D., & Sacks, P. G. (1998). Quantitation of chemopreventive synergism between (-)-epigallocatechin-3-gallate and curcumin in normal, premalignant and malignant human oral epithelial cells. *Carcinogenesis*, *19*, 419–424.

Khalil, A. A., Rahman, U., Khan, M. R., Sahar, A., Mehmood, T., & Khan, M. (2017). Essential oil eugenol: Sources, extraction techniques and nutraceutical perspectives. *RSC Advances*, *7*, 32669–32681.

Liberto, M., & Cobrinik, D. (2000). Growth factor-dependent induction of p21(CIP1) by the green tea polyphenol, epigallocatechin gallate. *Cancer Letters*, *154*, 151–161.

Livak, K. J., & Schmittgen, T. D. (2001). Analysis of relative gene expression data using real-time quantitative PCR and the 2(-Delta Delta C(T)) method. *Methods*, *25*, 402–408.

Loginov, V. I., Malyukova, A. V., Seryogin, Y. A., Hodyrev, D. S., Kazubskaya, T. P., Ermilova, V. D., … Braga, E. A. (2004). Methylation of the promoter region of the RASSF1A gene, a candidate tumor suppressor, in primary epithelial tumors. *Molekuliarnaia Biologiia (Moskva)*, *38*, 654–667.

Luo, K. L., Luo, J. H., & Yu, Y. P. (2010). (-)-Epigallocatechin-3-gallate induces Du145 prostate cancer cell death via downregulation of inhibitor of DNA binding 2, a dominant negative helix-loop-helix protein. *Cancer Prevention Research*, *101*, 707–712.

Manna, S., Mukherjee, S., Roy, A., Das, S., & Panda, C. K. (2009). Tea polyphenols can restrict benzo[a]pyrene-induced lung carcinogenesis by altered expression of p53-associated genes and H-ras, c-myc and cyclin D1. *Journal of Nutritional Biochemistry*, *20*, 337–349.

Mitra, S., Mazumder Indra, D., Bhattacharya, N., Singh, R. K., Basu, P. S., Mondal, R. K., … Panda, C. K. (2010). RBSP3 is frequently altered in premalignant cervical lesions: Clinical and prognostic significance. *Genes, Chromosomes & Cancer*, *49*, 155–170.

Morris, J., Moseley, V. R., Cabang, A. B., Coleman, K., Wei, W., Garrett-Mayer, E., & Wargovich, M. J. (2016). Reduction in promotor methylation utilizing EGCG (epigallocatechin-3-gallate) restores RXRα expression in human colon cancer cells. *Oncotarget*, *7*, 35313–35326.

Mukherjee, P., & Das, S. K. (1992). Partial characterization, progressive development and correlations of some neoplastic characters in 20-methylcholanthrene-induced transformed murine embryonal fibroblasts. *Cancer Letters*, *67*, 1–12.

Oya, Y., Mondal, A., Rawangkan, A., Umsumarng, S., Iida, K., Watanabe, T., … Suganuma M. (2017). Down-regulation of histone deacetylase 4, −5 and −6 as a mechanism of synergistic enhancement of apoptosis in human lung cancer cells treated with the combination of a synthetic retinoid, Am80 and green tea catechin. *Journal of Nutritional Biochemistry*, *42*, 7–16.

Pal, D., Banerjee, S., Mukherjee, S., Roy, A., Panda, C. K., & Das, S. (2010). Eugenol restricts DMBA croton oil induced skin carcinogenesis in mice: Downregulation of c-Myc and H-ras, and activation of p53 dependent apoptotic pathway. *Journal of Dermatological Science*, *59*, 31–39.

Pal, D., Sur, S., Mandal, S., Das, A., Roy, A., Das, S., & Panda, C. K. (2012). Prevention of liver carcinogenesis by amarogentin through modulation of G1/S cell cycle check point and induction of apoptosis. *Carcinogenesis*, *33*, 2424–2431.

Saha, P., Mandal, S., Das, A., Das, P. C., & Das, S. (2004). Evaluation of the anticarcinogenic activity of Swertia chirata Buch.Ham, an Indian medicinal plant, on DMBA-induced mouse skin carcinogenesis model. *Phytotherapy Research*, *18*, 373–378.

Sharp, T. V., Munoz, F., Bourboulia, D., Presneau, N., Darai, E., Wang, H. W., … Boshoff, C. (2004). LIM domains-containing protein 1 (LIMD1), a tumor suppressor encoded at chromosome 3p21.3, binds pRB and represses E2F-driven transcription. *Proceedings of the National Academy of Sciences of the United States of America*, *101*, 16531–16536.

Singh, B. N., Shankar, S., & Srivastava, R. K. (2011). Green tea catechin, epigallocatechin-3-gallate (EGCG): Mechanisms, perspectives and clinical applications. *Biochemical Pharmacology*, *82*, 1807–1821.

Sinha, S., Singh, R. K., Alam, N., Roy, A., Roychoudhury, S., & Panda, C. K. (2008). Frequent alterations of hMLH1 and RBSP3/HYA22 at chromosomal 3p22.3 region in early and late-onset breast carcinoma: Clinical and prognostic significance. *Cancer Prevention Research*, *99*, 1984–1991.

Stearns, M. E., & Wang, M. (2011). Synergistic effects of the green tea extract epigallocatechin-3-gallate and taxane in eradication of malignant human prostate tumors. *Translational Oncology*, *4*, 147–156.

Sur, S., Pal, D., Banerjee, K., Mandal, S., Das, A., Roy, A., & Panda, C. K. (2016). Amarogentin regulates self renewal pathways to restrict liver carcinogenesis in experimental mouse model. *Molecular Carcinogenesis*, *55*, 1138–1149.

Tao, L., Park, J. Y., & Lambert, J. D. (2015). Differential prooxidative effects of the green tea polyphenol, (-)-epigallocatechin-3-gallate, in normal and oral cancer cells are related to differences in sirtuin 3 signaling. *Molecular Nutrition & Food Research*, *59*, 203–211.

Weisburg, J. H., Weissman, D. B., Sedaghat, T., & Babich, H. (2004). In vitro cytotoxicity of epigallocatechin gallate and tea extracts to cancerous and normal cells from the human oral cavity. *Basic & Clinical Pharmacology & Toxicology*, *95*, 191–200.

Yang, C. S., Wang, X., Lu, G., & Picinich, S. C. (2009). Cancer prevention by tea: Animal studies, molecular mechanisms and human relevance. *Nature Reviews Cancer*, *9*, 429–439.

Yunos, N. M., Beale, P., Yu, J. Q., & Huq, F. (2011). Synergism from sequenced combinations of curcumin and epigallocatechin-3-gallate with cisplatin in the killing of human ovarian cancer cells. *Anticancer Research*, *31*, 1131–1140.

SUPPORTING INFORMATION

Additional supporting information may be found online in the Supporting Information section at the end of the article.

How to cite this article: Pal D, Sur S, Roy R, Mandal S, Kumar Panda C. Epigallocatechin gallate in combination with eugenol or amarogentin shows synergistic chemotherapeutic potential in cervical cancer cell line. *J Cell Physiol*. 2018;1–12. https://doi.org/10.1002/jcp.26900